Chapter 3
The Planetary Flybys

William A. Imbriale

The next era in Solar System exploration included flybys of the planets with spacecraft carrying scientific instruments designed to study the characteristics of the planets and intervening space. The Mariner series of spacecraft was designed to study the inner Solar System, and the two Voyager spacecraft were targeted for the outer planets.

Between 1962 and late 1973, The National Aeronautics and Space Administration's (NASA's) Jet Propulsion Laboratory (JPL) designed and built 10 spacecraft named Mariner to explore the inner Solar System [1]—visiting the planets Venus, Mars, and Mercury for the first time, and returning to Venus and Mars for additional close observations. The next-to-last mission, Mariner 9, became the first spacecraft to orbit another planet when it reached Mars for about a year of mapping and measurement. The final mission in the series, Mariner 10, flew past Venus before going on to encounter Mercury, after which it returned to Mercury for a total of three flybys.

The Mariners were all relatively small robotic explorers, each launched on an Atlas rocket with either an Agena or Centaur upper-stage booster, and each weighed less than half a ton (without onboard rocket propellant). Each of their missions was completed within a few months to a year or two, though one of them outlived its original mission and continued to send useful scientific data for three years.

The Voyager mission [2] was designed to take advantage of a rare geometric arrangement of the outer planets in the late 1970s and the 1980s. This layout of Jupiter, Saturn, Uranus, and Neptune (which occurs about every 175 years) allows a spacecraft on a particular flight path to swing from one

planet to the next without the need for large onboard propulsion systems. The flyby of each planet bends the spacecraft's flight path and increases its velocity enough to deliver it to the next destination. Using this "gravity assist" technique, the flight time to Neptune, with the rockets available at that time, was reduced from 30 years to 12. This mission has become known as The Grand Tour.

3.1 The Mariner Series

The Mariner series of missions were designed to be the first U.S. spacecraft to other planets, specifically Venus and Mars. This chapter focuses on the Venus and Mercury flybys, and Chapter 4 describes the Mars missions.

3.1.1 Mariners 1 and 2

Mariners 1 and 2 (Fig. 3-1) were nearly identical spacecraft developed to fly by Venus. The rocket carrying Mariner 1 went off-course during launch on July 22, 1962, and was blown up by a range safety officer about 5 minutes into flight. A month later, Mariner 2 was launched successfully on August 27, 1962, sending it on a 3-1/2-month flight to Venus. On the way, it measured for the first time the solar wind, a constant stream of charged particles flowing outward from the Sun. It also measured interplanetary dust, which was found to be scarcer than predicted. In addition, Mariner 2 detected high-energy charged particles coming from the Sun, including several brief solar flares, as well as cosmic rays from outside the Solar System. As it flew by Venus on December 14, 1962, Mariner 2 scanned the planet with infrared and microwave radiometers, revealing that Venus has cool clouds and an extremely hot surface. Because the bright, opaque clouds hide the planet's surface, Mariner 2 was not outfitted with a camera.

3.1.1.1 Mariner Antennas. The radio frequency (RF) subsystem [3,4] employed four antennas for the various in-flight communications requirements. Reception of ground-transmitted signals was through the Command Antenna System; a dipole antenna and a turnstile antenna mounted above and below the outboard end of a solar panel. Both antennas relayed the received 890-MHz energy to the communications transponder through a flexible coaxial cable.

Prior to spacecraft midcourse maneuver, an omnidirectional antenna located at the apex of the spacecraft structure transmitted 960-MHz signals to the ground. A separate L-band cavity amplifier provided power to the antenna. Following midcourse maneuver and after the attitude of the spacecraft had been corrected, the radio frequency (RF) power was radiated by a high-gain directive antenna located at the base of the spacecraft hex structure. A separate cavity amplifier also drove this antenna. The high-gain antenna (HGA) was nested at

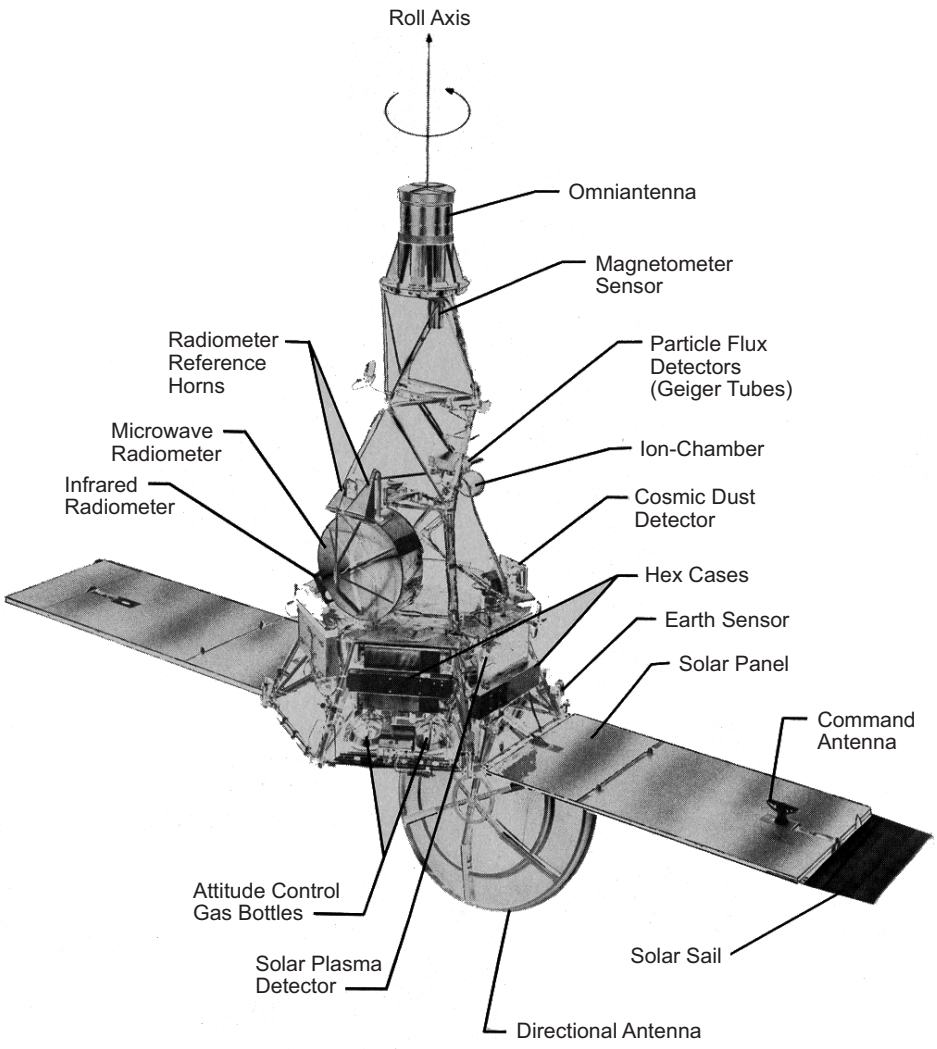

Fig. 3-1. Mariner 2 spacecraft.

the base of the spacecraft structure until midcourse maneuver, when it swung into position and faced the Earth. RF power was fed from the cavity amplifier to the HGA through flexible coaxial cables and a rotary joint. The cavity amplifiers were switched to provide either an omnidirectional pattern or an Earth-directed lobe.

A substantial portion of the antenna system was inherited from the Ranger Spacecraft. The omni antenna, for early flight telemetry, was the Ranger disc-cone antenna. The directional HGA used the Ranger 1 feed modified for circular polarization and a Ranger type parabolic reflector. This feed was then also used on Rangers 6 and 7. Radio-frequency continuity between the HGA

and the communications system during relative motion of the antenna and bus was provided by a Ranger 1-type coaxial rotary joint and associated cabling.

Omni antenna. The omni antenna, having been taken directly from the Ranger configuration, required no design work, but some structural strengthening was necessary. The omnidirectional antenna was located at the apex of the spacecraft structure and was driven by a separate L-band cavity amplifier.

Command antenna subsystem. The command antenna subsystem consisted of a turnstile antenna mounted on the backside of the solar panel and a dipole antenna mounted on the forward side of the solar panel (Fig. 3-2). To split the power between the two antennas, a directional coupler was used, with the dipole being driven 6 dB below that of the turnstile.

High-gain antenna. Requirements for the Mariner HGA design were the following:

1) The existing paraboloidal reflector had to be used with a minimum of modifications.
2) The design had to provide an efficient circularly polarized feed at 960 MHz.
3) The feed structure had to be compatible with the adapter diaphragm of the Ranger-Agena B vehicle.

A feed design was quickly accomplished by modifying the existing Ranger 1 configuration. The modification involved the replacement of the linearly polarized dipole elements with circularly polarized turnstile elements consisting of two dipoles oriented 90 deg from each other and 45 deg from the balun slot on the outer conductor. In the design, circular polarization was achieved by the phase quadrature of the essentially equal currents flowing in the crossed dipoles when one dipole was cut appropriately shorter than that required for resonance and the other appropriately longer than that required for resonance.

Several focal-length positions were examined in order to optimize the gain. At each position, the element lengths were adjusted to produce nearly circular polarization, meeting the criterion that the gain variation versus incident linear polarization angle be less than 0.2 dB. The 1-dB and 3-dB beamwidths of the antenna were 10.3 and 16.5 deg, respectively. Absolute gain relative to right-hand circular polarization (RHCP) of the antenna was measured to be 20.0 ±0.5 dB. Gain variation of the antenna versus incident linear polarization angle (ellipticity) was measured to be 0.33 dB.

3.1.2 Mariner 5

The Mariner 5 spacecraft was originally built as a backup to Mariner 4, a Mars craft launched in 1964. When Mariner 4 completed its mission

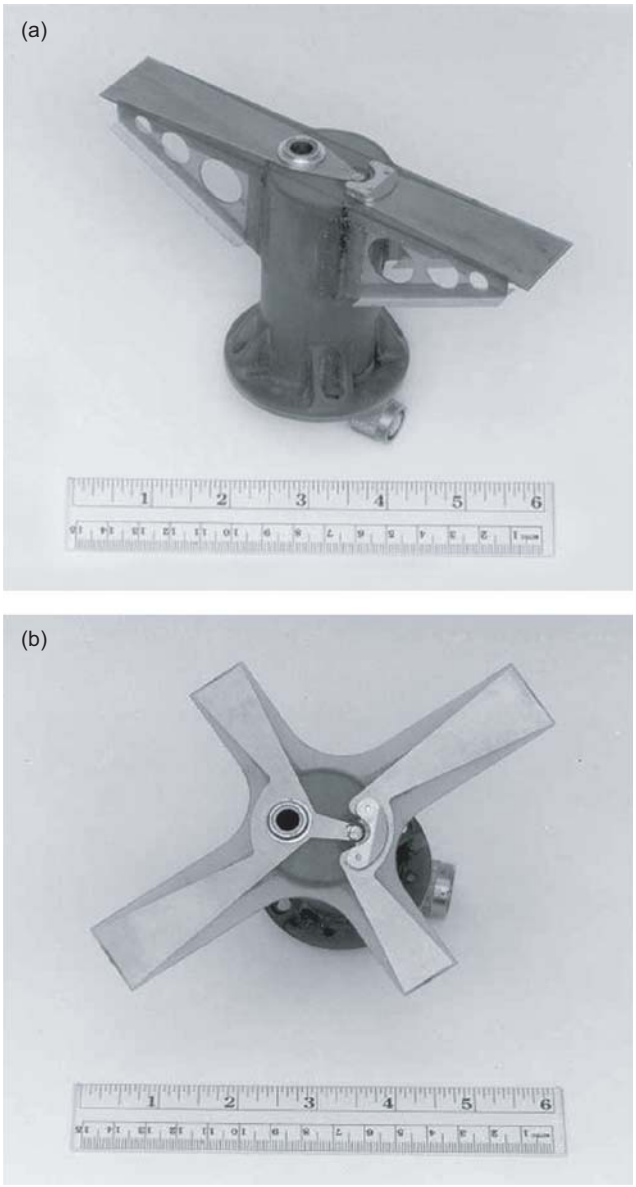

Fig. 3-2. Mariner 2 command antennas: (a) dipole and (b) turnstile.

successfully, the backup was rechristened Mariner 5 and reoutfitted for a flyby of Venus. Launched from Cape Canaveral, Florida, in June 1967, Mariner 5 (Fig. 3-3) flew within about 4,000 km (approximately 2,500 miles) of Venus some four months later. Mariner 5's flight path following its Venus encounter brought it closer to the Sun than any previous probe.

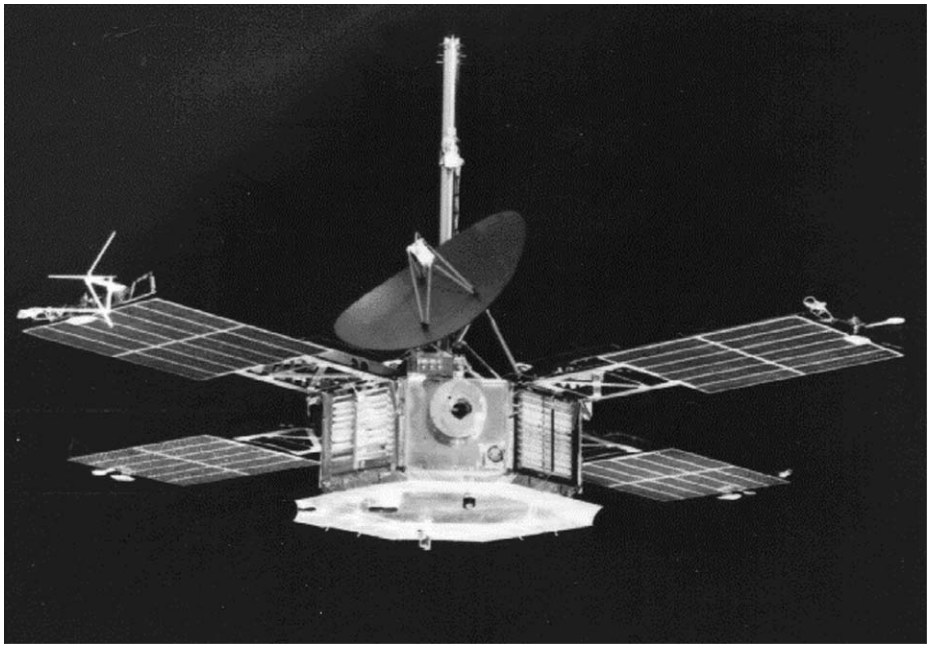

Fig. 3-3. Mariner 5 spacecraft.

The spacecraft antenna subsystem included a low-gain antenna (LGA), an HGA, and their transmission lines [5]. The function of the LGA was to receive commands from Earth and to transmit telemetry to Earth during the first half of the mission and during midcourse maneuver. The primary function of the HGA was to transmit telemetry to Earth during the last half of the transfer orbit and for a period after planetary encounter. The Earth-look angles were somewhat different than those for the Mariner 4 mission. Look angles for Venus continued away from the low-gain peak after encounter, while those at Mars reversed and retraced through the low-gain beam. Thus, the trajectories put the Earth-look angles on the opposite sides of the spacecraft. This placement of these angles would not have been a difficult problem if only telemetry and command requirements had to be met, since the encounter range of Venus was only 80 million km, whereas it was 222 million km for Mars in 1965. Hence, for the Venus encounter, the antenna gain required was about 9 dB less than that for Mariner 4 at Mars. If this antenna gain, then, was the only requirement, a relatively small antenna could have been packaged on the opposite side of the Mariner 4 type-spacecraft to accomplish the encounter antenna coverage. However, the S-band occultation experiment had to be considered as a key element, and for this, a nominal peak gain of 21.5 dB was required, which was approximately the gain required for telemetry return from Mars by Mariner 4.

This fact sized the Mariner 5 HGA to something approximately the same as the Mariner 4 HGA.

Since an antenna of this size would be impossible to position between the spacecraft and the Agena or between the bus and the shroud adapter, the antenna would have had to be stowed above the bus during launch and deployed after planetary injection, or the solar axis of the spacecraft would have had to be reversed. Of these two choices, the reversal of the solar axis appeared to be not only inherently the most reliable but also the easiest to implement.

In this configuration, the Mariner 4 LGA could be used without changes for Mariner 5, since the cone angle variations of Earth with time from launch to loss of LGA signal would now be similar. Clock-angle variations were not of significance in the LGA selection, since its pattern was essentially symmetrical about the roll axis.

Hence, S-band antennas made for Mariner 4 were used for Mariner 5 with only minor changes. The LGA consisted of an RHCP mode launcher in the base of a 2.1-m-long, 0.10-m-diameter circular aluminum waveguide, with a crossed slot radiator and a ground-plane system at the other end (Fig. 3-4). The base of the antenna was mounted in a fixed position on the spacecraft structure with the waveguide extending parallel to the spacecraft Z-axis.

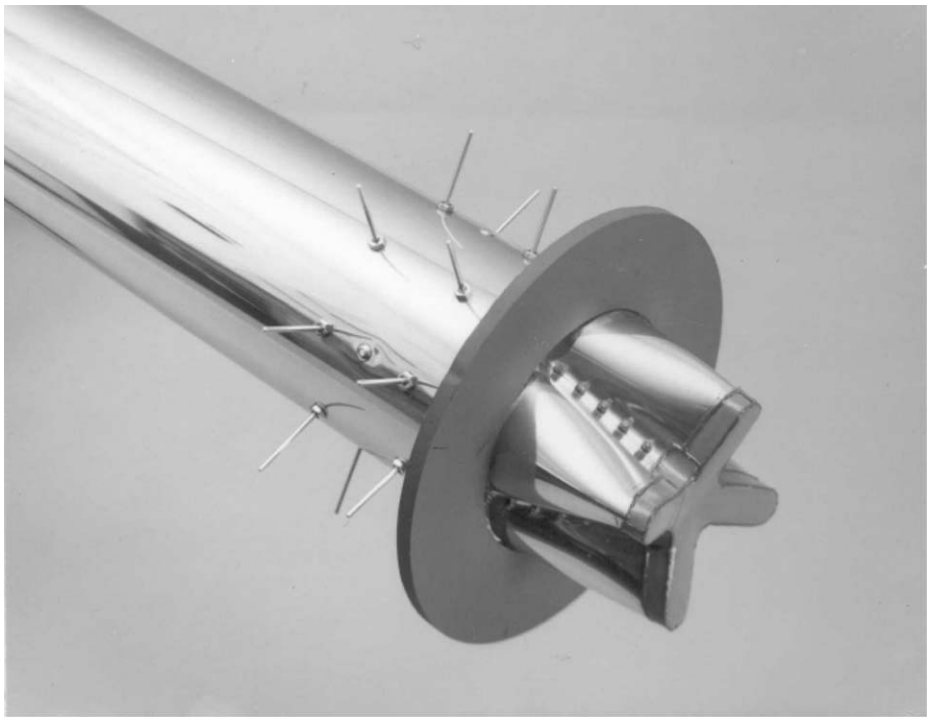

Fig. 3-4. Mariner 5 low-gain antenna.

The HGA consisted of a reflector and feed (Fig. 3-5). The reflector was a sectoral paraboloid, with an elliptic aperture that had a major axis of 1.17 m and a minor axis of 0.53 m. The feed was an array of two turnstile elements driven in phase through a stripline power divider and matching network. The HGA was right-hand circularly polarized. A fiberglass feed support truss joined the feed and reflector, an antenna support truss joined the reflector to the spacecraft, and a section of rigid coax tubing (supported by the feed and antenna support trusses) passed from the feed through the reflector.

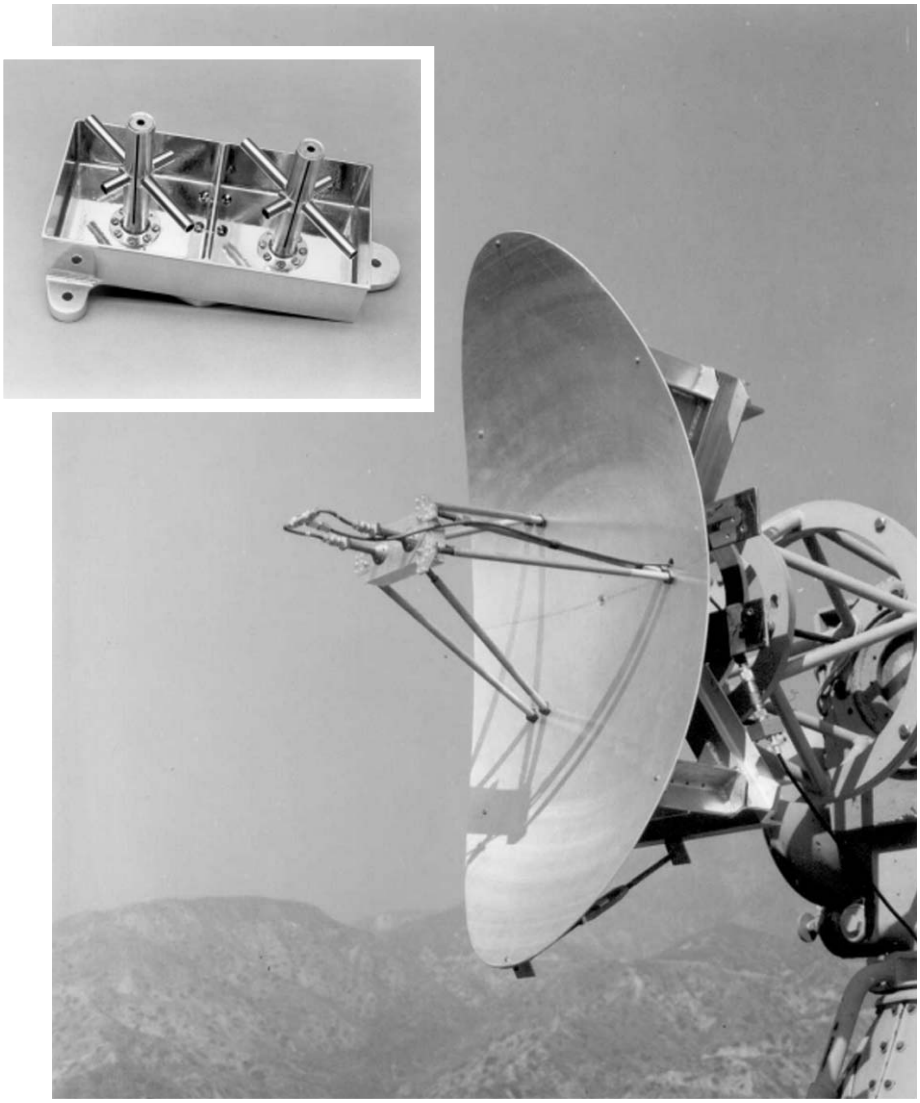

Fig. 3-5. Mariner 5 breadboard high-gain antenna.

Unlike Mariner 4, the Mariner 5 HGA had two separate positions to accommodate the occultation experiment. For a fixed on-board antenna, the occultation experiment required two peaks with approximately 21.5 dB nominal gain, each spaced 53 deg apart in the plane containing the earth track with sufficient cross Earth track to account for out-of-plane bending of the occultation whiskers. Various antenna studies narrowed the logical choice to the Mariner 4 HGA with its 23.2-dB peak gain and 2.06:1 beamwidth aspect ratio, along with a simple one-step position change to be made while the spacecraft was behind the planet. This choice would allow optimum pointing of the antenna back along the Earth track when entering occultation, then, allow it to be placed to a second position behind the planet allowing optimum pointing for the outgoing occultation. The offset angle chosen for the first position of the HGA was a compromise between occultation optimization and telemetry return to Earth after encounter in the event that the antenna pointing angle change did not occur. Hence, the first offset angle was –8.2 deg, while the exit occultation offset was 9.5 deg.

Changes made to accommodate the two positions included the addition of a new mounting interface structure and revision of the coaxial cabling between the antenna and the electronic cases. A tuned mismatch was inserted in the LGA transmission line as a result of an interferometer problem on Mariner 4 caused by insufficient isolation between the high-gain and low-gain antennas. A detailed discussion of this problem may be found in [5].

3.1.3 Mariner 10

With Mariner 10, JPL engineers embarked on an experiment with an ingenious way of traveling through the Solar System using the gravity of one planet to help propel the craft on to the next destination—somewhat like a series of bank shots in a game of billiards [6].

With the scorched inner planet Mercury as its ultimate target, the final Mariner pioneered the use of a “gravity assist” swing by the planet Venus to bend its flight path. Using a near-ultraviolet filter, it produced the first clear pictures of the Venusian chevron clouds and performed other atmospheric studies before moving to the small, airless, cratered globe of Mercury. Here a fortuitous gravity assist enabled the spacecraft to return at six-month intervals for close mapping passes over the planet, covering half the globe (Mercury’s slow rotation left the other half always in the dark when Mariner 10 returned).

The S/X-band antenna subsystem requirements provided for transmission and reception of S-band signals between the DSN and the Mariner spacecraft and for transmission of X-band signals from the spacecraft to the DSN [7,8]. The subsystem consisted of one HGA, one LGA, an HGA coupler, plus the necessary RF transmission lines and associated connectors. The HGA requirements were to downlink S-band (2295 + 5 MHz) and X-band (8415 + 20

MHz) using an RHCP signal. The gain requirements were S-band 27.6 ±0.25 dB and X-band 38.2 ±0.4 dB. The LGA requirements were to uplink and downlink S-band (2115 ±5 MHz receive and 2295 ±5 MHz transmit). The polarization was RHCP, and the minimum gains at mercury encounter when the Sun was acquired were receive –4.1 dB and transmit –3.1 dB.

A schematic of the antenna subsystem is shown in Fig. 3-6. The HGA was a steerable parabolic dish 54 in. (137.2 cm) in diameter with a focal length of 21.6 in. (54.88 cm). It used a collocated S-and X-band focal point feed where the S-band feed was an annular cavity, and the X-band feed was an open-ended circular waveguide. The LGA was a boom-mounted biconical antenna with the boom used as an air-dielectric coaxial transmission line. It was fixed mounted after deployment from stowed position, but it had a post-Mercury encounter redeployment capability. The transmission lines used 50-Ω semi-rigid coax, and the deployment and articulating joints used 50-Ω flexible coax.

There was some heritage from the earlier Mariner missions for the HGA dish materials, but the feed was new, and the LGA was a new design patterned after a lunar orbiter LGA design but with simplified feed and thermal expansion joint. The antenna subsystem weight was 7.24 lb (3.3 kg).

Pictures of the HGA feed are shown in Figs. 3-7 and 3-8. Studies were made of the vertex-to-feed distance, and the outer cup depth and the measured data for S-band are shown in Fig. 3-9. The selected design was 22.2 in. (56.4 cm) focal distance and 1.6 in. (4.1 cm) cup. The measured gains were 27.6 dB at S-band and 38.74 dB at X-band.

The Mariner LGA configuration is shown in Fig. 3-10. Typical patterns compared to the specification are shown in Fig. 3-11.

3.2 Voyager Mission to the Outer Planets

The Voyager mission [2] was designed to take advantage of a rare geometric arrangement of the outer planets in the late 1970s and the 1980s. This layout of Jupiter, Saturn, Uranus, and Neptune, which occurs about every 175 years, allows a spacecraft on a particular flight path to swing from one planet to the next without the need for large onboard propulsion systems. The flyby of each planet bends the spacecraft's flight path and increases its velocity enough to deliver it to the next destination. Using this "gravity assist" technique, the flight time to Neptune was reduced from 30 years to 12.

While the four-planet mission was known to be possible, it was deemed to be too expensive to build a spacecraft that could go the distance, carry the instruments needed, and last long enough to accomplish such a long mission. Thus, the Voyagers were funded to conduct intensive flyby studies of Jupiter and Saturn only. More than 10,000 trajectories were studied before choosing the two that would allow close flybys of Jupiter and its large moon Io, and

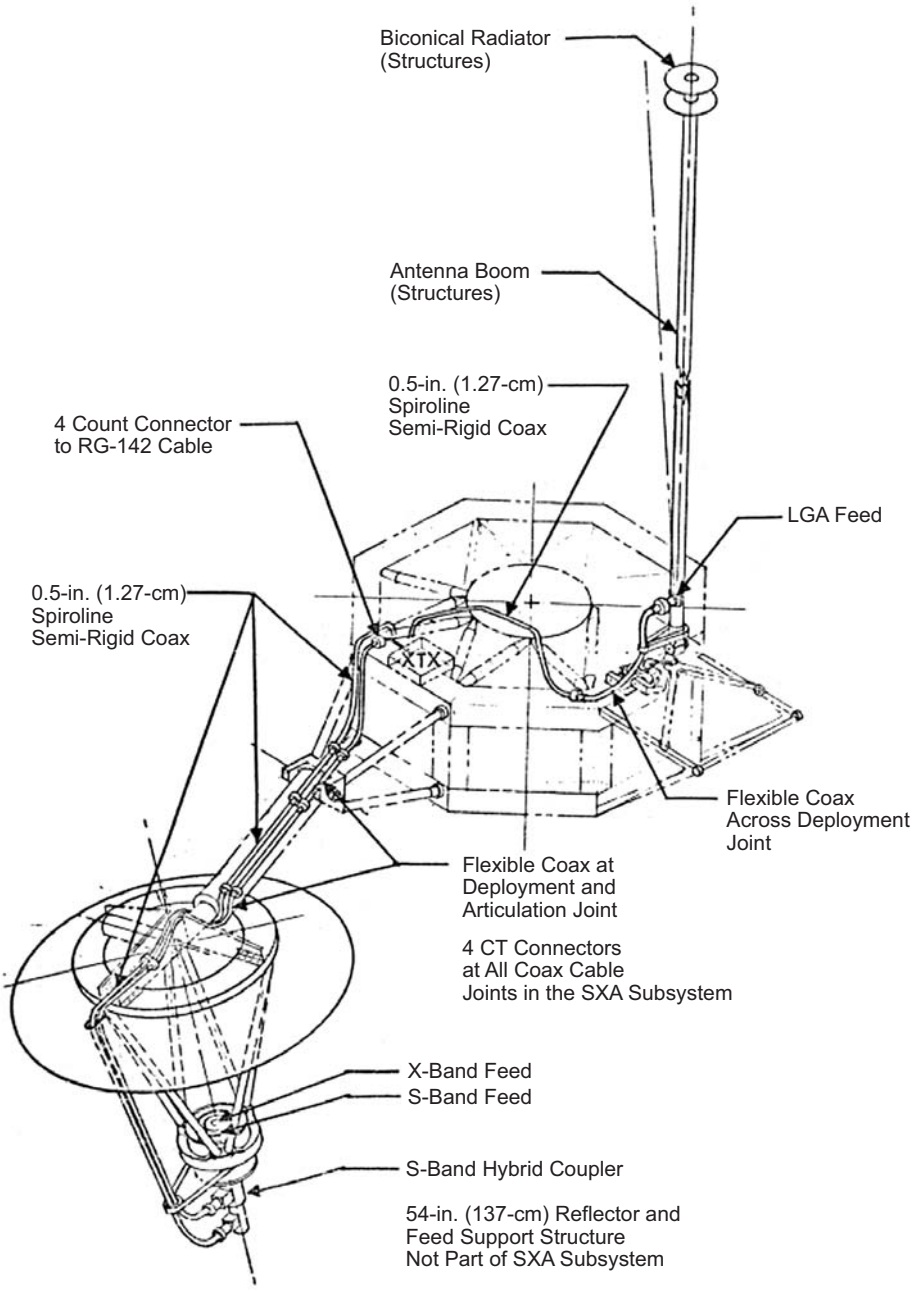

Fig. 3-6. Mariner 10 antenna subsystem (CT = coil terminal).

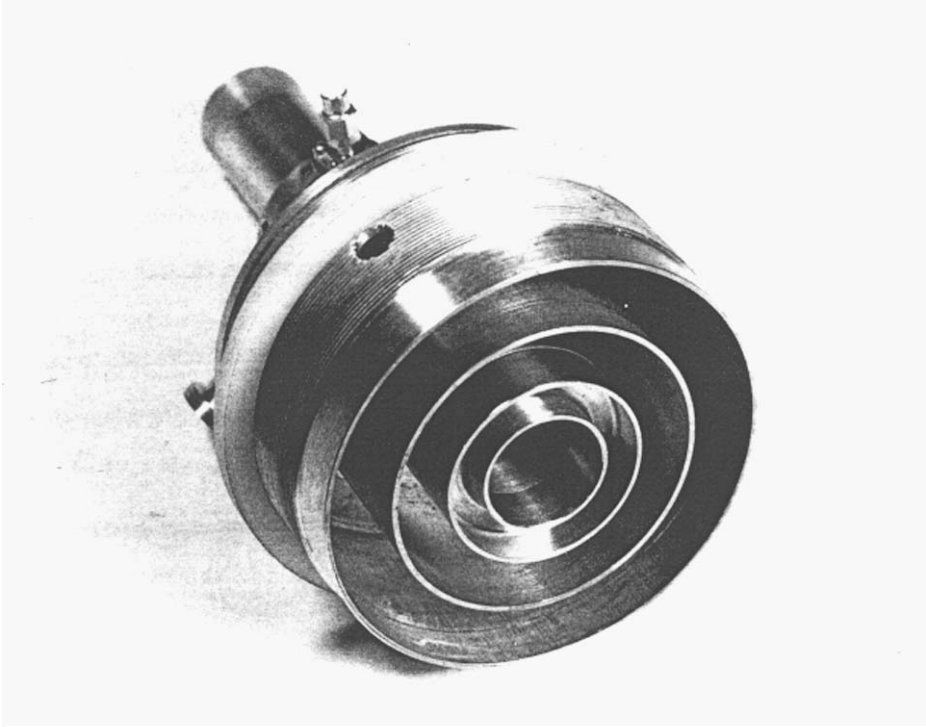

Fig. 3-7. Mariner 10 HGA feed.

Saturn and its large moon Titan. The chosen flight path for Voyager 2 also preserved the option to continue on to Uranus and Neptune.

From the NASA Kennedy Space Center at Cape Canaveral, Florida, Voyager 2 was launched first, on August 20, 1977; Voyager 1 was launched on a faster, shorter trajectory on September 5, 1977. Both spacecraft were delivered to space aboard Titan-Centaur expendable rockets. The prime Voyager mission to Jupiter and Saturn brought Voyager 1 to Jupiter in 1979 and Saturn in 1980, while Voyager 2 flew by Jupiter in 1979 and Saturn in 1981. Voyager 1's trajectory, designed to send the spacecraft closely past the large moon Titan and behind Saturn's rings, bent the spacecraft's path inexorably northward out of the ecliptic plane—the plane in which most of the planets orbit the Sun. Voyager 2 was aimed to fly by Saturn at a point that would automatically send the spacecraft in the direction of Uranus.

After Voyager 2's successful Saturn encounter, it was shown that Voyager 2 would likely be able to fly on to Uranus with all instruments operating. NASA provided additional funding to continue operating the two spacecraft and authorized JPL to conduct a Uranus flyby. Subsequently, NASA also authorized the Neptune leg of the mission, which was renamed the

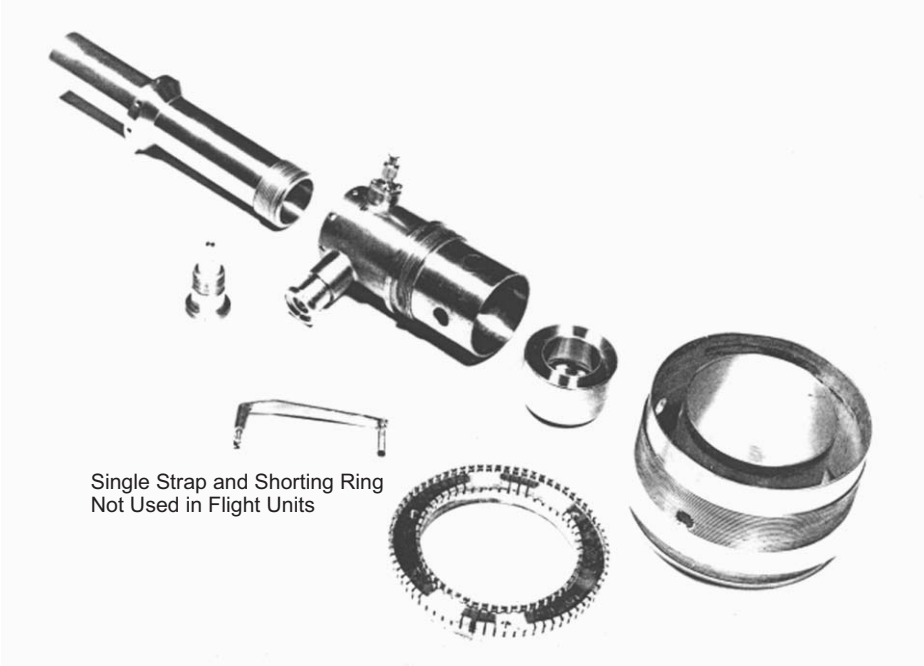

Fig. 3-8. Mariner 10 HGA feed, exploded view.

Voyager Neptune Interstellar Mission. It should be pointed out, however, that although Voyager 2 was targeted to fly by Uranus and Neptune, the telecommunications link was only designed for operation at Jupiter and Saturn. Since it was not possible to change the spacecraft, significant improvements in the ground portion of the link were necessary for a successful mission at Uranus and Neptune. A description of the many improvements to the ground antenna system can be found in [9]. It included, among other things, an addition of another 34-m antenna subnet, increasing the size of the existing 64-m antennas to 70-m, and arraying 34-m and 70-m antennas.

Voyager 2 encountered Uranus on January 24, 1986, returning detailed photos and other data on the planet, its moons, its magnetic field, and its dark rings. Voyager 1, meanwhile, continued pressing outward, conducting studies of interplanetary space. Eventually, its instruments may be the first of any spacecraft to sense the heliopause—the boundary between the end of the Sun's magnetic influence and the beginning of interstellar space.

Following Voyager 2's closest approach to Neptune on August 25, 1989, the spacecraft flew southward, below the ecliptic plane and onto a course taking it, too, to interstellar space. Reflecting the Voyagers' new transplanetary destinations, the project name was changed to the Voyager Interstellar Mission.

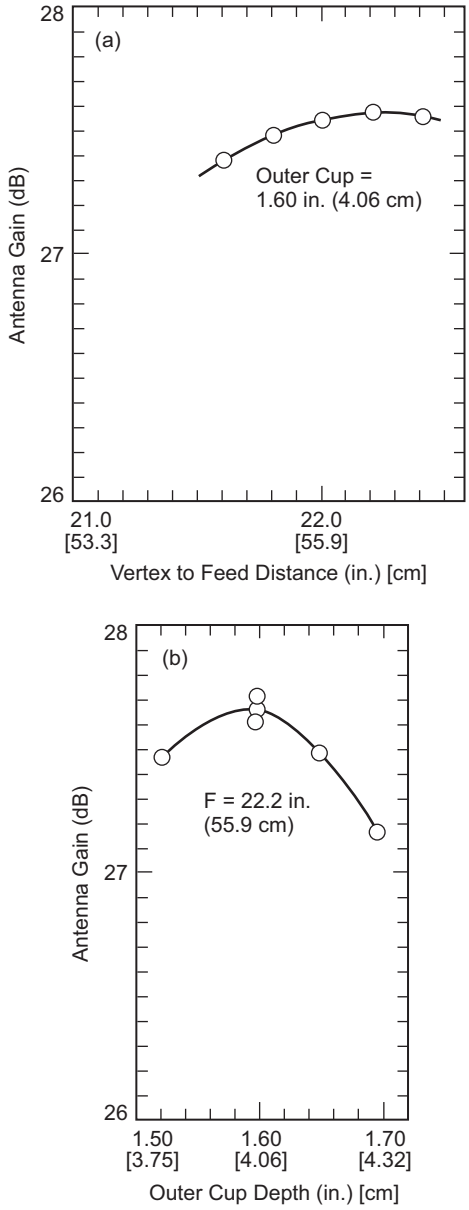

Fig. 3-9. Mariner 10 HGA S-band gain measurements (measurements obtained using linear standard gain horn): (a) vertex to feed distance and (b) outer cup depth.

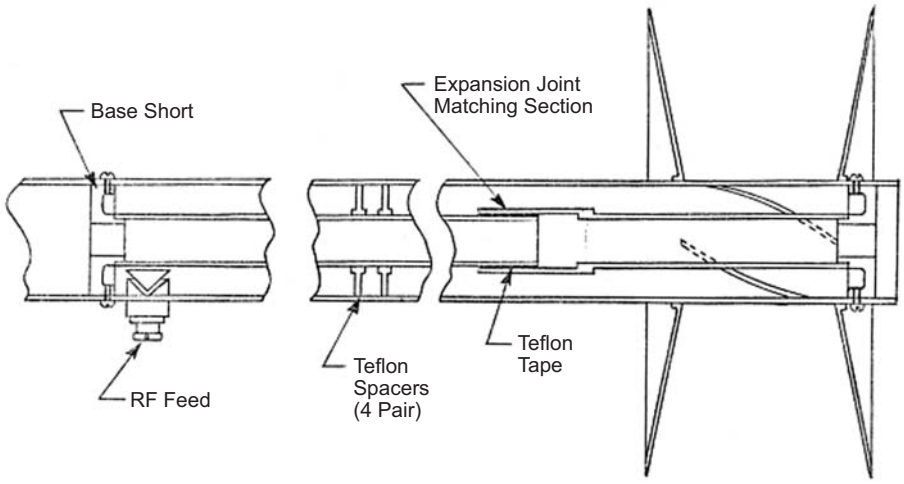

Fig. 3-10. Mariner 10 LGA configuration.

Voyager 1 is now leaving the Solar System, rising above the ecliptic plane at an angle of about 35 degrees at a rate of about 520 million kilometers (about 320 million miles) a year. Voyager 2 is also headed out of the Solar System, diving below the ecliptic plane at an angle of about 48 degrees and a rate of about 470 million kilometers (about 290 million miles) a year.

Both spacecraft will continue to study ultraviolet sources among the stars, and the fields and particles instruments aboard the Voyagers will continue to search for the boundary between the Sun's influence and interstellar space. The Voyagers are expected to return valuable data for two or three more decades. Communications will be maintained until the Voyagers' nuclear power sources can no longer supply enough electrical energy to power critical subsystems.

3.2.1 Voyager S-/X-Band Antenna Subsystem

The Voyager spacecraft (Fig. 3-12) S-/X-band antenna subsystem (SXA) is required to (1) receive S-band signals from the DSN and conduct them to the radio frequency subsystem (RFS), (2) transmit S-band signals from the RFS to the DSN, and (3) transmit X-band signals from either RFS X-band traveling wave tube assembly (TWTA) to the DSN [10,11].

A schematic diagram of the SXA is shown in Fig. 3-13. It consists of an HGA, an LGA, transmission lines (including waveguide and X-band power monitors), and RF power probes located on the HGA main reflector and the LGA cavity.

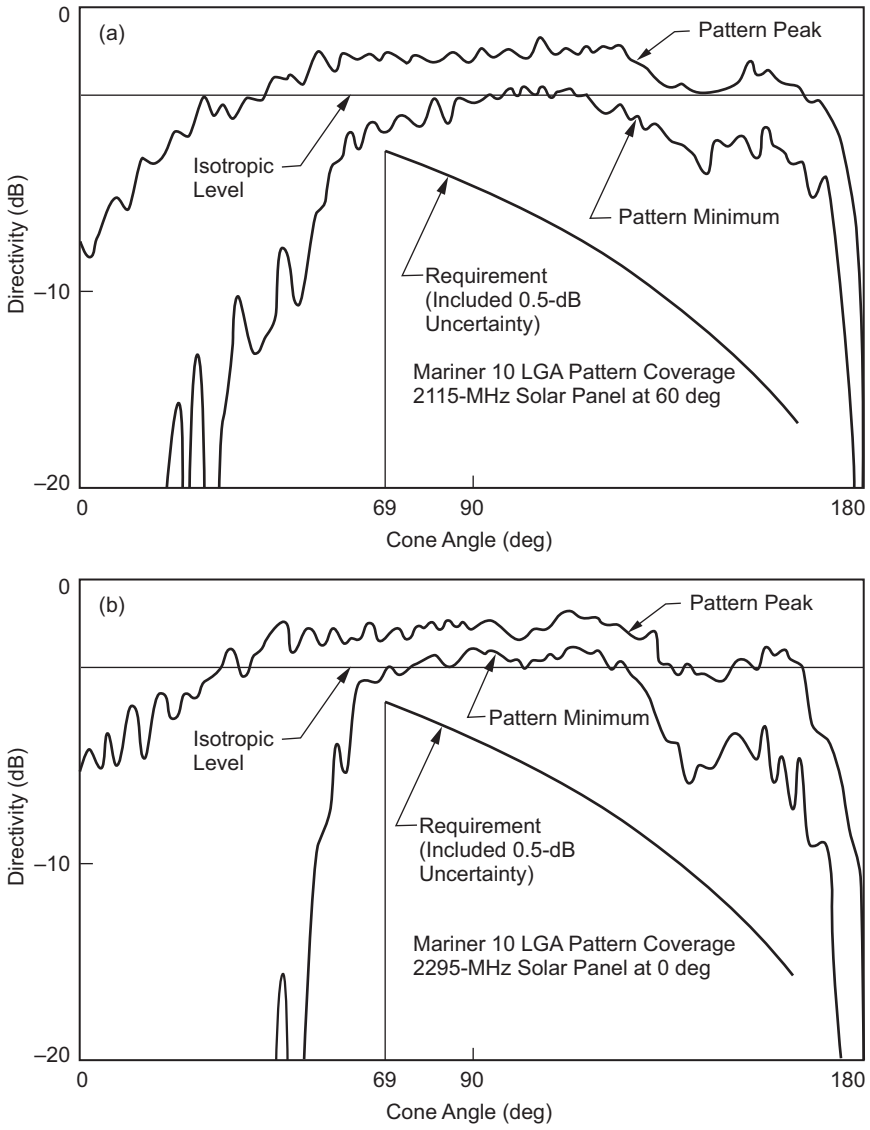

Fig. 3-11. Mariner 10 LGA patterns: (a) 2115 MHz and (b) 2295 MHz.

3.2.2 Requirements

The HGA consists of a paraboloidal reflector with a 3.66-m (12-ft.) diameter circular aperture and suitable S- and X-band feeds. The X-band feed utilizes dual shaped Cassegrain optics, and the S-band feed utilizes a prime focus feed. A frequency selective subreflector (FSS) reflects the X-band signal and passes the S-band signal. The HGA has a focal length to diameter (F/D) ratio of 0.338. The HGA is RHCP and operates over the frequency ranges of

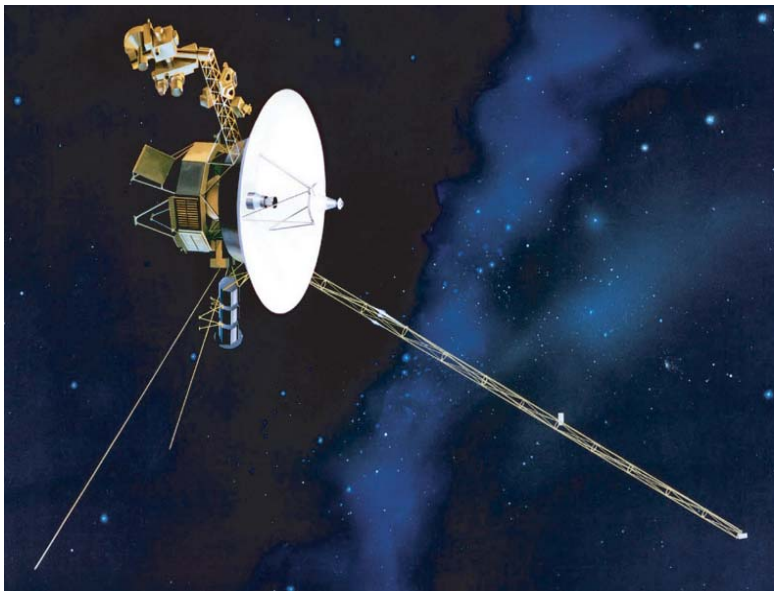

Fig. 3-12. The Voyager spacecraft.

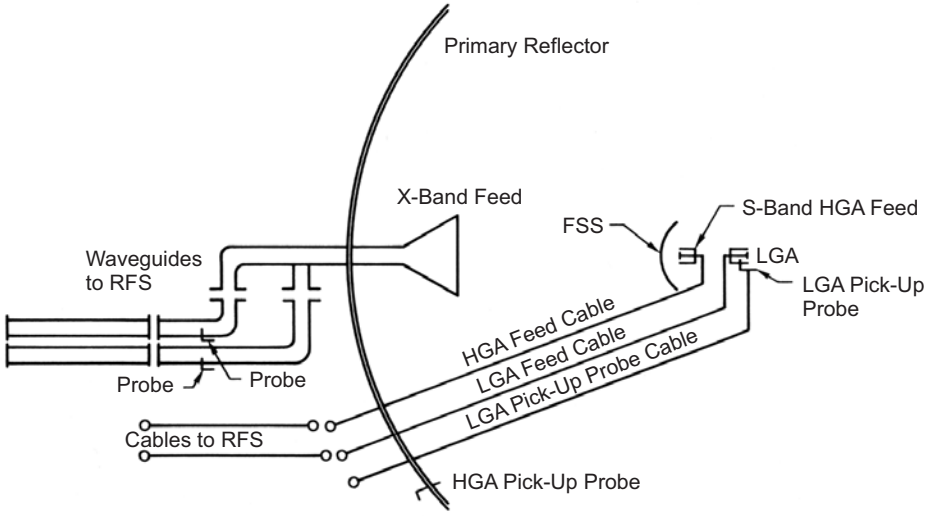

Fig. 3-13. Voyager SXA subsystem.

2115 ±5 and 2295 ±5 MHz. It also operates over the frequency range of 8422 ±20 MHz, with a dual polarized feed that yields a right-hand or left-hand circularly polarized wave from the HGA depending on which of its input ports is excited by the RFS. S-band signals are received by the HGA at 2115 ±5 MHz and routed to the RFS receiver. S-band signals at 2295 ±5 MHz from the RFS

S-band transmitter are radiated via the HGA. X-band signals at 8422 ±20 MHz from the RFS X-band transmitter are radiated via the HGA.

The LGA radiates a circularly polarized, broadbeam pattern directly to Earth. The LGA requirements are summarized in Table 3-1.

3.2.3 Voyager High-Gain Antenna

Since a 3.66-m reflector was the largest solid reflector diameter that could fit into the nose cone fairing without deployment, it was desirable to have the highest aperture efficiency possible. A high-efficiency dual-reflector system generally requires that (1) most of the feed energy be intercepted by the reflectors (i.e., low spillover), and (2) the field in the aperture of the main reflector be distributed as uniformly as possible. Ordinarily, reduction of spillover requires tapering the aperture distribution, and a uniform aperture distribution generally involves substantial spillover. Consequently, optimum performance traditionally involves a compromise that has limited efficiencies of conventional systems to about 55–60 percent. The shaped dual-reflector concept permits the apparent contradiction between the two requirements for high efficiency to be overcome with the following rationale: a feed is selected with a high taper at the edge of the subreflector to minimize forward spillover; the subreflector profile is designed to distribute the highly tapered energy uniformly over the aperture of the main reflector. By designing for constant aperture illumination (see Section 1.2.4), the classical hyperboloid subreflector is transformed into an empirical contour with a smaller radius of curvature than a hyperboloid in the central section to deflect more of the rays to the outer part of the main reflector. Thus, there is little spillover and, at the same time, a nearly uniform aperture distribution. The main reflector must then be slightly

Table 3-1. Voyager low-gain antenna requirements.

Parameter	Requirement
Frequency bands	2115 ±5 MHz (receive) 2295 ±5 MHz (transmit)
Power handling	120 W continuous wave (CW)
Polarization	RHCP
Axial ratio	2115 MHz band: ≤6 dB for ±90-deg cone angle; ≤2 dB on boresight
	2295 MHz band: ≤11 dB for ±90-deg cone angle; ≤2 dB on boresight
Boresight gain (at input connector) pattern	≥7.5 dBi for 2115-MHz band ≥7.6 dBi for 2295-MHz band
VSWR	≤1.2 : 1 for both bands

reshaped from its original paraboloidal contour to produce a constant-phase distribution

The HGA was dual-shaped for optimum efficiency at X-band (see Fig. 3-14). The dichroic subreflector is transparent to radiation from an S-band prime-focus horn nestled behind it. At S-band, the main reflector differs little from a paraboloid. The focus of the resultant best-fit paraboloid was chosen as the prime focus for the S-band feed.

3.2.3.1 X-band Feed. The X-band feed [12] is required to illuminate the subreflector with circularly symmetric, circularly polarized energy of a prescribed pattern shape with constant pattern phase. A subreflector edge illumination level of 17.5 dB below the boresight pattern level was chosen as the best comprise between the –25 dB optimum gain edge illumination and typical feed phase patterns, which have large rates of change past the –17.5 dB points.

The subreflector shape was calculated based on a computer-predicted pattern for the dual-mode horn baseline feed. Therefore, the computer-predicted

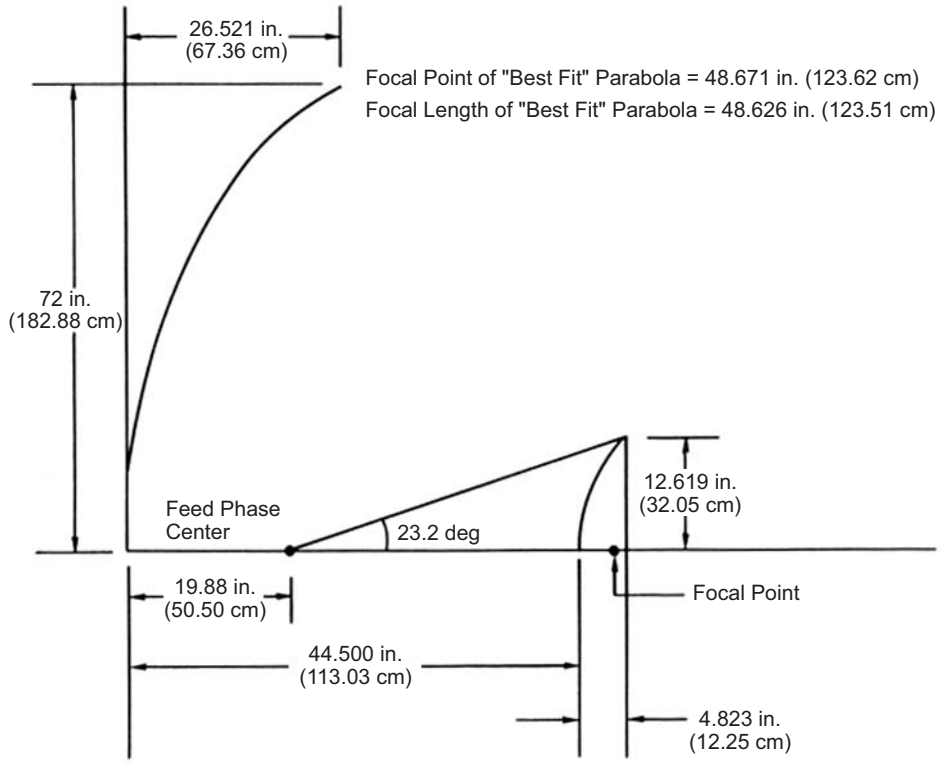

Fig. 3-14. Voyager HGA geometry.

pattern was the design goal for the X-band breadboard feed. The X-band feed requirements are summarized in Table 3-2.

3.2.3.2 Trade-off Studies. Circular polarization consists of two spatially orthog-onal E-field components 90 deg out of time phase. Good circular polarization for a given feed horn pattern can occur only if the pattern is closely matched in orthogonal planes and has nearly identical phase-centers in orthogonal planes. Radiation patterns in the dominant transverse electric (TE_{11}) circular waveguide mode have narrower E-planes than H-planes due to the more nearly uniform E-field aperture distribution in the E-plane. Radiation in the transverse magnetic (TM_{11}) mode, in phase with the TE_{11} mode at the horn aperture, increases E-plane beamwidth and reduces E-plane sidelobe levels without affecting H-plane radiation patterns.

Potter [13] found that TM_{11} power in the proper ratio to the TE_{11} mode could nearly equalize E- and H-plane beamwidths. Ludwig [14] found that radiation from the TE_{12} and TM_{12} modes in combination with the TE_{11} mode and TM_{11} mode could produce beams with fairly flat tops and steep skirts, or shaped beams with nearly equal E-and H-plane beamwidths. The combination of the TE_{11} and TM_{11} mode is the hybrid HE_{11} mode, and the combination of TE_{12} mode and TM_{12} mode is the HE_{12} mode. An antenna radiating in the HE_{11} and HE_{12} modes is a dual hybrid-mode antenna.

Therefore, the X-band feed candidate antennas considered were the dual mode horn, the corrugated horn, and the dual hybrid-mode horn. The operation of each of these type horns is described in the following paragraphs.

3.2.3.2.1 Dual Mode Horn. TM_{11} mode power is generated at the step change in circular waveguide size as a result of the boundary condition requiring tangential E-fields to vanish at a perfectly conducting wall. The ratio of waveguide diameter left of the step to the waveguide diameter to the right of the step, or step ratio, determines the ratio of TM_{11} mode power to TE_{11} mode power to the right of the step.

Table 3-2. Voyager X-band feed specifications.

Parameter	Required Performance
Frequency band	8422 ±20 MHz
Polarization	RHCP and LHCP from two different input ports
Power handling	105 W CW
VSWR	≤1.2 : 1.0
Axial ratio	≤1.0 dB*

* Internal specification. The X-band system axial ratio specification is 1.5 dB on the boresight axis.

The waveguide size at the left of the step was chosen such that the TM_{11} mode is below cutoff. The TM_{11} mode and TE_{11} mode propagate with different phase velocities, and therefore change their relative phase relationship in the horn flare section.

The phasing section also yields a differential phase shift between the two modes. Its length was adjusted during testing so that the two modes are in phase at the aperture. For the Voyager antenna, the phasing section length was determined experimentally because, although the differential phase shift between the two modes in the flare section could be calculated, the computer program did not calculate the initial phase relationship at the step. The dependence on the absolute length of the phasing and flare sections for proper performance limits the dual mode horn bandwidth to between 5 and 10 percent.

3.2.3.2.2 Corrugated Horn. The corrugated horn utilizes TE_{11} and TM_{11} mode radiation to equalize E- and H-plane beamwidths. The bandwidth limitations of the stepped dual mode horn are overcome by using corrugations to generate TM_{11} mode power in a distributed manner along the flare section, thus eliminating the phase difference between the two modes. The corrugations, which are $\lambda/4$ deep, may be viewed as providing equal boundary conditions in the E- and H-planes. There should be enough corrugations per wavelength such that the corrugated wall performs as an anisotropic surface.

3.2.3.2.3 Dual Hybrid-Mode Horn. It is possible to add hybrid modes in a corrugated waveguide analogously to adding individual TE and TM modes in a smooth waveguide. The TM_{11}, TE_{12}, and TM_{12} modes are generated at the step and propagate through the corrugated flare section, unlike in the dual-mode horn that attenuates the HE_{12} mode in its phasing section. The combination of the two hybrid modes can produce radiation patterns with nearly equal and shaped E- and H-plane beams over a narrow band. JPL [15] has tested a dual-hybrid-mode horn from 8.3 GHz to 8.6 GHz and has developed computer analysis programs for the horn.

3.2.3.2.4 Choice of Dual-Mode Horn as X-Band Feed. The Voyager X-band bandwidth is 0.475 percent, which is well within the 5-percent bandwidth capability of the dual-mode horn; therefore, the wideband, corrugated horn design offers no advantage over the dual-mode horn and is more expensive to fabricate. Although the beam-shaping property of the dual-hybrid-mode horn could yield some advantages over the dual-mode horn, the use of dual-shaped optics for the reflector system negates that advantage. Also the increased complexity, fabrication cost, weight, and blockage at S-band of the dual-hybrid-mode horn over the dual-mode horn makes the dual-mode horn the clear choice as the X-band feed.

3.2.3.2.5 Detailed Design of the Voyager X-Band Feed Horn. Figure 3-15 gives the dimensions of the feed, the polarizer, and the orthomode transducer, and the following describes the process used to determine the design. Some of the parameters were determined empirically, as the computer programs used at that time did not provide a complete solution. The program described in Section 1.2.2 could be used today to completely design the horn without the need for measurements.

Aperture diameter. The addition of the TM_{11} mode radiation pattern to the TE_{11} mode pattern broadens the E-plane beam to match the H-plane beam, without affecting the H-plane beam; therefore, the diameter of the dual-mode horn was chosen based on the H-plane pattern of a dominant mode horn. A 4.905-in. (12.46-cm) diameter (~3.5 wavelengths) aperture yields a –17.5-dB pattern taper at the 23.2-deg subreflector edge cone angle. A computer program computed the radiation pattern for a TM_{11}/TE_{11} mode voltage ratio of 10.626, both modes in phase, and a 4.905-in. (12.46-cm) diameter aperture. This computer pattern was then used as the design goal for the feed because the subreflector shape was determined from the computer-predicted feed pattern.

Phasing section design. The phasing section diameter, 2.05 in. (5.21 cm), was chosen to be 20 percent above the TM_{11} mode cutoff diameter at 8422 MHz. The closer the TM_{11} mode is to cutoff, the more effective is a given length of phasing section in providing the required TE_{11} to TM_{11} mode differential phase shift to put the two modes in phase at the aperture. However, if the TM_{11} mode is too close to cutoff, its guide wavelength varies radically with frequency, thus severely limiting the antenna bandwidth. A phasing section diameter 20 percent above the TM_{11} mode cutoff diameter is a

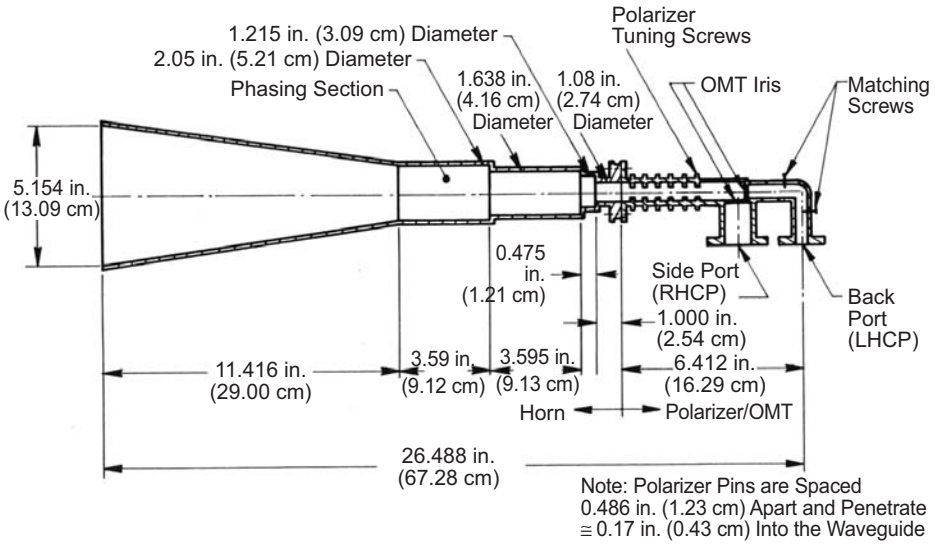

Fig. 3-15. Voyager HGA X-band feed horn cross section and dimensions.

compromise between phasing section effectivity and antenna bandwidth. Also, a small diameter phasing section is effective in attenuating modes of higher order than TM_{11} generated at the step.

Step ratio. The E-plane pattern of the dual-mode horn is only an approximation to the H-plane pattern. One design factor in a dual-mode horn is the pattern level at which the E- and H-plane coincide. The feed breadboard step ratio was chosen such that the –10 dB points coincide. Designing the step so that the E- and H-plane beams coincide at the –10 dB pattern levels causes the beams to be in close agreement for the 23.2-deg portion subtended by the subreflector. Breadboard tests determined that a step ratio of 0.799 optimized the beamwidth match.

Input matching section. A quarter-wave transformer and a linear taper were each considered for matching the input or feed waveguide impedance to the waveguide impedance at the step section input. The linear taper was not used because it was 3 in. (7.62 cm) longer than the quarter-wave transformer and more suited to wideband applications.

3.2.3.3 X-Band Performance Summary. The performance of the antenna system at X-band is summarized in Table 3-3.

3.2.4 Voyager S-Band Feed and Low-Gain Antenna Design

The S-band feed and LGAs [16] are back-to-back in the SXA system (Fig. 3-13). The S-band feed is required to illuminate the main reflector with

Table 3-3. Voyager X-band performance summary at 8422 ±20 MHz.

RF Parameter		Specification	Measured Performance	
			RHCP	LHCP
Gain (dB)		≥48.3	47.96	47.98
Efficiency (η) (percent)		64.9	60.0	60.2
Axial ratio (on-axis) (dB)		≤1.5	0.6	0.6
3-dB beamwidth (deg)		≥0.5	0.58	0.58
10-dB beamwidth (deg)		≥0.9	0.97	0.97
First sidelobe angle from boresight (deg)		≥0.9	0.9	0.9
First sidelobe level (dB)		>15.0	13 to 17	13 to 17
VSWR	8402 MHz	≤1.2 : 1	1.06 : 1	1.17 : 1
	8422 MHz		1.03 : 1	1.05 : 1
	8442 MHz		1.03 : 1	1.06 : 1
Isolation (dB)	8402 MHz	>20	20.5	
	8422 MHz		19.5	
	8442 MHz		18.6	

circularly polarized power in a circularly symmetric pattern with a prescribed edge taper. The feed position is the focal point of the best-fit parabolic approximation of the main reflector. The LGA radiates a circularly polarized, broadbeam pattern directly to Earth. Fig. 3-16 is the LGA pattern specification. Tables 3-4 and 3-5 summarize the LGA and S-band feed design requirements. A calculated prime focus fed parabola efficiency curve versus reflector edge illumination shows that the S-Band HGA efficiency will be nearly identical for feed patterns rolling off from –8 dB through –11 dB with respect to boresight at the 73-deg cone angle subtended by the main reflector. This wide range of feed patterns for high efficiency performance of the HGA S-band system allowed use of an antenna design that meets both the LGA patterns and S-band feed specifications, thereby reducing system cost and complexity. The sense of circular polarization is the only difference between the two antennas. Because the S-band feed and the LGA are of the same design, they shall hereafter be referred to as the S-band feed/LGA.

3.2.4.1 Design Summary. The initially proposed S-band feed and LGA was a self-phased crossed dipole matched by a triple tuner. Concern about the thermal stability and reliability of the triple-stub tuner resulted in a change of the S-Band feed/LGA to a hybrid-fed crossed dipole (HFCD). The HFCD design, Fig. 3-17, provides the four-way equal power split and 0, –90, –180, –270 deg phase progression required for circular polarization from a 180-deg ring hybrid feeding two 90-deg "over and under" couplers. The four outputs of the two 90-deg hybrids are connected to the four printed circuit radiating elements by sections of 0.141-in. (0.36-cm) diameter semi-rigid cables. The cables run the length of the square, beam-shaping cavity. An alternate approach to feeding the four radiating elements would have been to use a single 90-deg hybrid feeding the two orthogonal pairs of radiating elements; the opposite elements dividing current using a quarter-wave balun.

The balun design, however, required close feed-cable spacing and a cross strap between opposite radiating element pairs; both susceptible to voltage breakdown. The radiating cavity dimensions are such that the S-band feed pattern at 73 deg illuminates the main reflector edge at –11 dB. This edge illumination is in the maximum efficiency region for the primary reflector.

The breadboard LGA design is an S-band feed element with two 1/2-in. (1.27-cm) spaced, 6-in. (15.24-cm) diameter conductive disks conforming to the radiating cavity wall and with the upper disk at the level of the radiating element. The upper disk forms a ground plane that narrows the pattern half-power beamwidth from ~94 deg to ~77 deg and increases the gain from ~6.3 dBi to ~8.0 dBi, so that the LGA gain specification can be met. The lower disk, upper disk, and cavity wall roughly form a quarter-wave, short-circuited channel that "chokes off " edge currents and reduces the back lobe from –18 dB

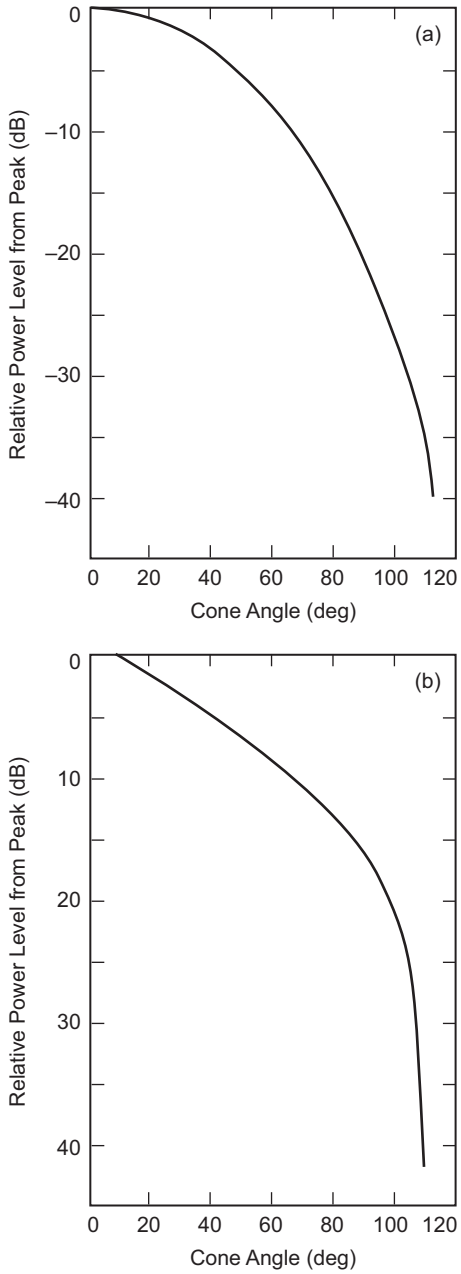

Fig. 3-16. Voyager low-gain antenna pattern performance criteria for: (a) 2115 ±5 MHz and (b) 2295 ±5 MHz.

Table 3-4. Voyager low-gain antenna requirements.

Parameter	Requirement
Frequency bands	2115 ±5 MHz (receive) 2295 ±5 MHz (transmit)
Power handling	120 W CW
Polarization	RHCP
Axial ratio	2115 MHz band: ≤6 dB For ±90-deg cone angle; ≤2 dB On boresight
	2295 MHz band: ≤11 dB For ±90-deg cone angle; ≤2 dB On boresight
Boresight gain (at input connector) pattern	≥7.5 dBi for 2115-MHz band ≥7.6 dBi for 2295-MHz band
VSWR	≤1.2 : 1.0 for both bands

Table 3-5. Voyager S-band feed requirements.

Parameter	Requirement
Frequency bands	2115 ±5 MHz (receive) 2295 ±5 MHz (transmit)
Power handling	120 W CW
Polarization	LHCP
Axial ratio	≤1.5 dB average within ± 73-deg cone angle
Pattern rolloff	–8 dB through –11 dB with respect to boresight at 73-deg cone angle (space taper is 4 dB)

to –23 dB. This back-lobe reduction decreases the effect of the primary reflector collimating the LGA back radiation and generating interference ripple in the LGA pattern.

3.2.4.2 Radiation Performance of the LGA in the Presence of the Primary Reflector. As discussed above, a choke channel was added to the LGA that reduced the back radiation level from –18 dB to –23 dB. This reduced, but did not eliminate the effect of interference from the primary reflector. Interference ripples are due to the primary reflector collimating the back radiation of the LGA and producing an interference pattern. To reduce the effect of primary reflector interference on the LGA pattern, the LGA was moved as far from the primary reflector focal point as system considerations would allow, thus defocusing the back radiation and reducing the level of the interference signal. Spacing ranging from the original initial baseline of 55.5 in. (141 cm) (the primary reflector subtends at a 136.15-deg angle from the LGA) to 64.5 in.

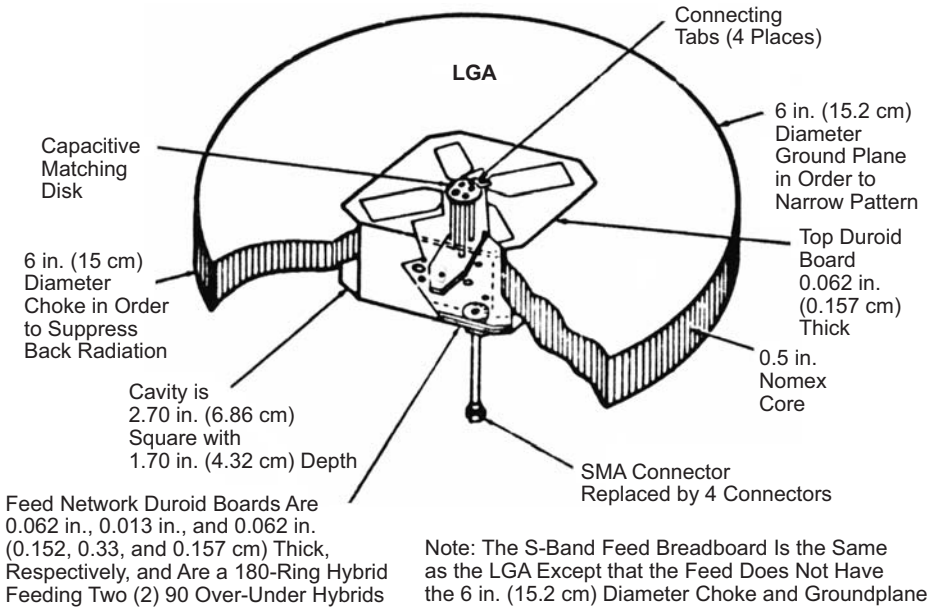

Fig. 3-17. Voyager S-band feed and LGA outline diagram.

(163.8 cm) (the primary reflector subtends a 124.4-deg angle from the LGA) was studied. The nominal spacing chosen as the prototype baseline, based on a compromise between RF performance and system considerations, was 62.9 in. (159.8 cm) (126.4 deg of LGA angle subtended by the primary reflector). Figures 3-18 and 3-19 are LGA patterns at the 62.9-in. (159.8-cm) spacing at 2115 MHz and 2295 MHz, respectively.

3.2.4.3 HGA S-band Performance Summary. Table 3-6 summarizes the S-band HGA final performance with 0.75-in. (1.9-cm) metal struts at one half the radius with the hybrid-fed cross dipole feed. The only significant parameter that the S-band feed system fails to meet is the gain at the transmit frequency (2295 MHz). The gain includes the Spiroline cable loss of 0.4 dB at 2295 MHz and 0.35 dB at 2115 MHz.

3.2.4.4 S-band Strut/Feed Measurements. An extensive investigation was made of the S-band gain for various strut and S-band feed configurations. The HGA with the HFCD feed gave superior performance when compared to the HGA gain with the self-phased feed—particularly with the 3/4-in. (1.9-cm) metal struts. This higher gain was justification for changing the baseline feed from the self-phase dipole to the HFCD. The Kevlar struts configuration gave higher gain than the metal struts for all configurations. However, the Kevlar

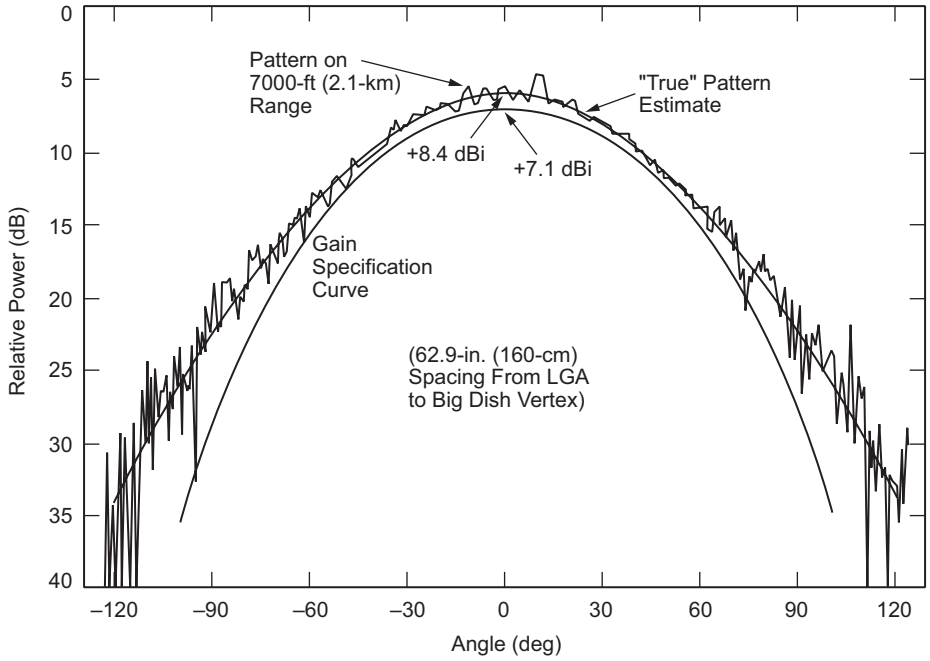

Fig. 3-18. Voyager 2215-MHz LGA pattern in the presence of the main reflector.

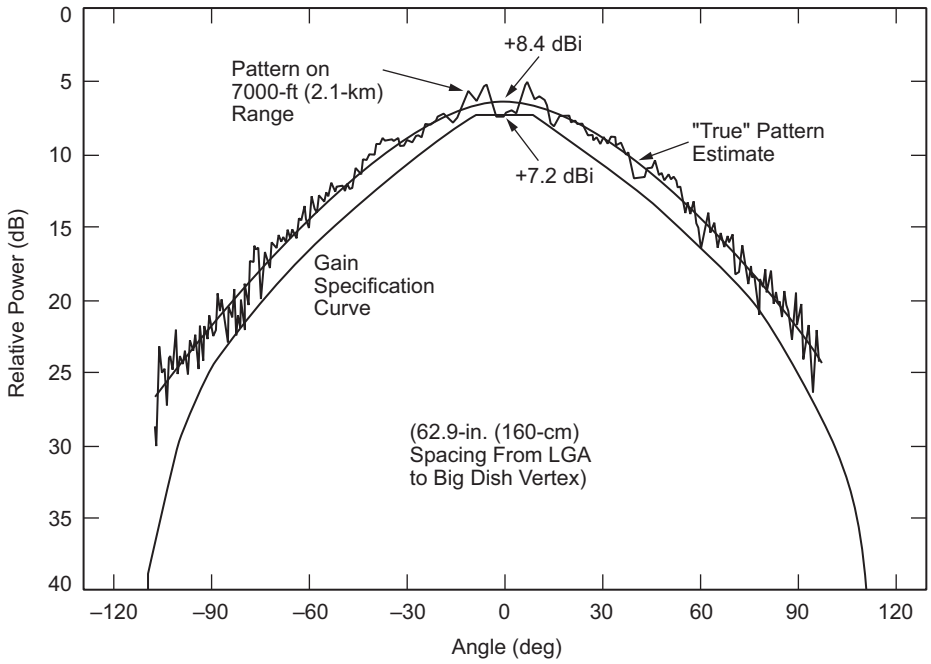

Fig. 3-19. Voyager 2295-MHz LGA pattern in the presence of the main reflector.

Table 3-6. Voyager HGA S-band performance summary with 0.75-in. (1.9-cm) metal struts.

RF Parameter	2115 MHz		2295 MHz	
	Specified	Measured	Specified	Measured
Gain (dB)	≥35.5	35.59	≥36.3	36.14
Efficiency (percent)	≥54.2	55.1	≥55.3	53.1
Axial ratio on-axis (dB)	≤2.0	0.5	≤1.5	0.8
3-dB beamwidth (deg)	2.8 ±0.3	2.8	2.6 ±0.3	2.5
10-dB beamwidth (deg)	5.2 ±0.3	4.8	4.8 ±0.3	4.3
First sidelobe angle from boresight (deg)	≤4.3	4.25	≥4.0	3.8
First sidelobe level (dB)	≤–20.0	–22.2 to –26.0	≤–20.0	–20.7 to –25.5
VSWR (at feed)	1.2 : 1	1.17 : 1	1.2 : 1	1.20 : 1

struts are a marginal mechanical design and consequently 3/4-in. (1.9-cm) graphite struts were selected as the baseline.

3.2.5 Voyager Frequency Selective Surface (FSS) Subreflector

The HGA utilizes prime focus/Cassegrainian geometry with an FSS to separate the frequencies. The FSS is transparent at low frequencies to allow prime focus operation, and it is reflective at the high frequency for Cassegrainian operation [17]. The FSS utilizes two layers of X-band aluminum resonant crossed dipoles printed on Mylar. The subreflector is constructed from a Kevlar/Nomex honeycomb-core sandwich (see Fig. 3-20). The size and geometry of the resonant dipoles are determined from flat panel tests (see Section 1.2.5), and the second layer is used to match the lower frequency. The performance goal was that the loss introduced at both frequency bands be less than 0.2 dB. Measured data confirmed a loss of <0.1 dB at S-band and between 0.1 and 0.2 dB at X-band. Figure 3-21 is a picture of the FSS subreflector.

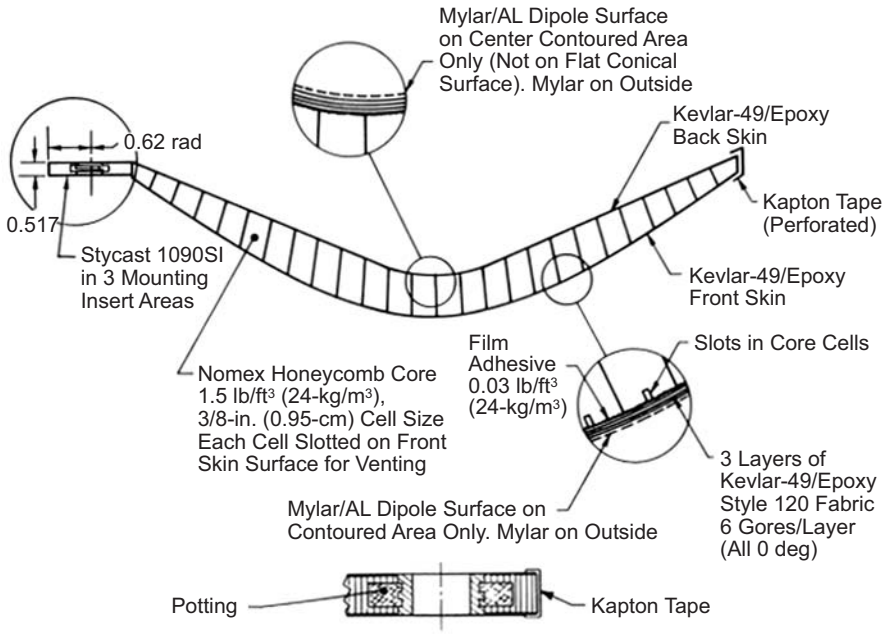

Fig. 3-20. Voyager FSS subreflector materials and construction.

Fig. 3-21. Voyager FSS subreflector.

References

[1] *NASA Facts: Mariner to Mercury, Venus and Mars* (web site), Jet Propulsion Laboratory, Pasadena, California, May 1996, accessed July 7, 2005. http://www.jpl.nasa.gov/news/fact_sheets/mariner.pdf

[2] *NASA Facts: Voyager Mission to the Outer Planets* (web site), Jet Propulsion Laboratory, Pasadena, California, May 1996, accessed July 7, 2005. http://www.jpl.nasa.gov/news/fact_sheets/voyager.pdf

[3] *The Mariner R Project: Progress Report September 1, 1961 – August 31, 1962*, JPL Internal Technical Report No. 32-353, Jet Propulsion Laboratory, Pasadena, California, also NASA-CR-135806, National Aeronautics and Space Administration, Washington, District of Columbia, January 1, 1963.

[4] J. N. Bryden, *Mariner (Venus '62) Flight Telecommunication System*, Technical Report No. 32-377, Jet Propulsion Laboratory, Pasadena, California, January 15, 1963.

[5] *Mariner Venus 67 Final Project Report*: Volume 1. *Launch through Midcourse Maneuver*, Technical Report 32-1203, Jet Propulsion Laboratory, Pasadena, California, June 15, 1968.

[6] *Past Missions - Mariner 10* (web page), Jet Propulsion Laboratory, Pasadena, California, accessed July 7, 2005. http://www.jpl.nasa.gov/missions/past/mariner10.html

[7] *S/X Band Antenna Subsystem FDR Data Package*, W.U. 33-2-1, Contract Mariner Venus/Mercury 1973 JPL Contract 953000, contract to Jet Propulsion Laboratory, Pasadena, California, Boeing Company, Seattle, Washington, November 4, 1971.

[8] MVM'73-4-2017, *Functional Requirement MVM'73 Spacecraft Equipment S/X-Band Antenna Subsystem*, MVM'73-4-2017 JPL Contract 953000, Contract to Jet Propulsion Laboratory, Pasadena, California, Boeing Company, Seattle, Washington, November 14, 1971.

[9] W. A. Imbriale, *Large Antennas of the Deep Space Network*, Chapters 5 and 6, John Wiley & Sons, Inc., Hoboken, New Jersey, 2003.

[10] *Functional Requirement Mariner Jupiter/Saturn 1977 Flight Equipment S/X-Band Antenna Subsystem*, MJS77-4-2017A, in JPL 618-205, *MJS77 Functional Requirements Book* (set of internal documents), Jet Propulsion Laboratory, Pasadena, California, February 3, 1977.

[11] *Mariner Jupiter/Saturn 1977 SXA Subsystem*, Vol. 1, *Critical Design Review*, Aeronutronic Ford Corporation, Palo Alto, California, November 1975.

[12] *Mariner Jupiter/Saturn 1977 S/X-Band Antenna Subsystem, Design Analysis Report*, Volume II *HGA/LGA Feed RF Analysis*, WDL Technical Report 5717, Philco-Ford Corporation, Palo Alto, California, March 18, 1975.

[13] P. D. Potter, *A New Horn with Suppressed Sidelobes and Equal Beamwidth*, Technical Report No. 32-354, Jet Propulsion Laboratory, Pasadena, California, February 25, 1963.

[14] A. C. Ludwig, *Antennas for Space Communication*, JPL SPS 37-33, Vol. IV, Supporting Research and Advanced Development, Jet Propulsion Laboratory, Pasadena, California, also NASA-CR-64605, National Aeronautics and Space Administration, Washington, District of Columbia, pp. 261–266, June 30, 1965.

[15] R. F. Thomas and D. A. Bathker, "A Dual Hybrid Horn Feedhorn for DSN Antenna Performance Enhancement," *The Deep Space Network Progress Report 42–22, May and June 1974*, Jet Propulsion Laboratory, Pasadena, California, pp. 101–108, August 15, 1974. http://ipnr.jpl.nasa.gov/progress_report/

[16] *Mariner Jupiter/Saturn 1977 S/X-Band Antenna Subsystem, Breadboard Development Report Addendum A*, WDL-TR5740, Aeronutronic Ford Corporation, Palo Alto, California, August 22, 1975.

[17] G. H. Schennum, "Frequency Selective Surfaces for Multiple-Frequency Antennas," *Microwave Journal*, pp. 56–59, March 1973.